한국해양공학회지 제22권 제2호, pp 1-6, 2008년 4월 (ISSN 1225-0767)

Numerical Analysis of Wave Field in OWC Chamber Using VOF Model

ZHEN LIU*, BEOM-SOO HYUN* AND JI-YUAN JIN*
*Division of Naval Architecture & Ocean Systems Engineering, Korea Maritime University, Busan, Korea
**College of Engineering, Ocean University of China, Qingdao, China.

KEY WORDS: Wave energy, OWC, Numerical wave tank, VOF model, Shape parameters

ABSTRACT: *Recently Oscillating Water Column (OWC) plants have been widely employed in wave energy conversion applications. It is necessary to investigate the chamber and optimize its shape parameters for maximizing air flow and energy conversion due to wave conditions. A 2D numerical wave tank based on a Fluent and VOF model is developed to generate the incident waves and is validated by theoretical solutions. The oscillating water column motion in the chamber predicted by the numerical method is compared with the available experimental data. Several geometric scales of the chamber are calculated to investigate the effect of the shape parameters on the oscillating water column motion and wave energy conversion.*

1. Introduction

Ocean energy can provide a clean renewable source of the electric power for coastal and island areas. Due to the advantages of simple converting technique and producing cost over other types of ocean energy, the wave energy conversion system is feasible to be established for the commercial power production. Plenty of wave energy absorption devices have been invented, and several of them have been utilized in the electricity generation. Recently, the oscillating water column (OWC) type has been widely employed in the application for the wave energy conversion. It consists of a partially submerged air chamber with an opening in the front skirt. Waves can force the water column in the chamber to oscillate, which can produce the bi-directional airflow through the air turbine. Therefore, the wave energy will be converted to the low pressure pneumatic power.

A number of experimental and numerical investigations about OWC wave energy conversion devices have been performed. Falnes (1980) and Evan (1982) developed the theory of OWC wave energy absorption. Physical model with different bottom slopes was constructed and tested in a wave tank under regular wave conditions by Wang (2002). Liang et al. (2003) studied the air chamber performance under incident wave heights and nozzle ratios experimentally. Hong et al. (2007) performed an experiment concentrating on the effects of several shape parameters of OWC chamber in wave energy absorbing capability. You (1993) presented a boundary element method to study the influence of coastal topography and the harbor shape on the oscillations of the OWC plant. Wang (2002) employed the linear wave theory by using a boundary element method based on 3D shallow water Green's function to investigate the effects of the bottom slope on the hydrodynamic performance of onshore wave-power devices. Hong et al. (2004) calculated the motions and time-mean horizontal drift forces of floating backward-bent duct buoy wave energy absorbers in regular waves taking account of the oscillating surface pressure due to the pressure drop in the air chamber above the oscillating water column within the scope of the linear wave theory.

It should be noted that the experimental investigations are restricted by the laboratory conditions, costs and scale effects. The above numerical simulations just focused on the wave and water column motion, however, the water-air interaction and air flow motion which is extremely important, can not be predicted directly.

In the present study, a 2D numerical wave tank is established to simulate the regular waves based on the commercial Computational Fluid Dynamis software Fluent 6.2.16. The Reynolds Averaged Navier-Stokes (RANS) equations coupled with VOF model are adopted to calculate the wave propagation in the numerical tank and oscillation in the chamber. VOF model has been proved that it can simulate the complex wave structure interaction effectively and track the free water surface precisely. The 2D numerical wave tank is validated by the theoretical solutions and the prediction of oscillating water column motion is compared with the available experimental

교신저자 현범수: 부산광역시 영도구 동삼동 1번지
051-410-4308 bshyun@hhu.ac.kr

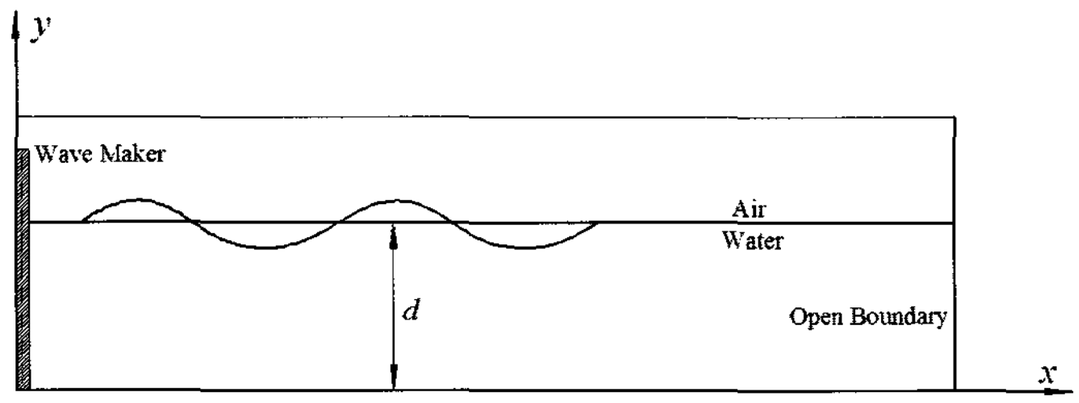

Fig. 1 Schematic of numerical wave tank

data. Various geometry scales of the chamber will be investigate to demonstrate the effects of shape parameters on the wave field, water column oscillation in the chamber and wave energy conversion.

2. Numerical Wave Tank

2.1 Governing equations

The schematic of a 2-D numerical wave tank is shown in Fig. 1. The propagating waves are generated by the wave maker plate at the left end, and an opening boundary is set at the other end.

The governing equations are the continuity equation and RANS equations for an impressible fluid:

$$\frac{\partial u_i}{\partial x_i}=0 \tag{1}$$

$$\frac{\partial u_i}{\partial t}+u_i\frac{\partial u_i}{\partial x_i}+u_j\frac{\partial u_i}{\partial x_j}=-\frac{1}{\rho}\frac{\partial p}{\partial x_i}+f_{x_i}+\frac{\partial}{\partial x_j}[\upsilon\frac{\partial u_i}{\partial x_j}-\overline{u_i'u_j'}] \tag{2}$$

where x_i , u_i represent the coordinate directions and corresponding velocity components; ρ, p, ν, f_{x_i} are the fluid density, the fluid pressure, the kinematic viscosity coefficient, and the body force, respectively.

The component $\overline{u_i'u_j'}$ defined as the Reynolds stress induces a new turbulence model to close the equations. The standard $k-\epsilon$ model widely used in engineering application, is employed in this study to demonstrate the turbulence effect in the wave motion.

The tracking of the interface between the air and water phases is accomplished by the volume of fluid (VOF) method (Hirt and Nichols, 1981). The volume fractions of water and air in the computational cell sum to unity. If the volume fraction of water is defined as a_w , then the following three conditions are possible: (1). a_w= 0, the cell is empty of water; (2). a_w = 1, the cell is full of water. (3). 0 < a_w < 1, the cell contains the interface. The volume fraction a_w is computed as:

$$\frac{\partial a_w}{\partial t}+\frac{\partial(a_w u_i)}{\partial x_i}=0 \tag{3}$$

In addition, the face fluxes through the computational cells are obtained as the geometric reconstruction approach. The interface between two fluids is calculated by the piecewise-linear scheme, which assumes the linear slope in each cell.

2.2 Numerical solutions

The regular linear wave is employed in the investigation of this paper, and the motion of the piston wave maker is determined from the following equation:

$$x(t)=\frac{S_0}{2}(1-e^{-\frac{5t}{2T}})\sin\omega t \tag{4}$$

where S_0 is the maximum displacement of the wave maker; T is the period of incident wave, and $\omega=2\pi/T$.

On the opening boundary, the Sommerfeld radiation boundary condition (Sommerfeld, 1949), which has good capability of linear wave absorption, can be written as:

$$\frac{\partial\phi}{\partial t}+c\frac{\partial\phi}{\partial x}=0 \tag{5}$$

where ϕ is velocity potential and c is wave velocity. Substituting Eq. (5) for the dynamic boundary condition of the free surface in the linear wave theory, the relation between the horizontal velocity component and the free surface elevation is obtained:

$$u=\frac{g\eta}{c} \tag{6}$$

where $u=\partial\phi/\partial x$ denotes the horizontal velocity, η the free surface elevation and g the gravity acceleration. The wave absorption can be performed by controlling the motion of the opening boundary.

The motion of the wave generating and absorbing boundaries can be achieved by defining UDF (user-defined function) programs. Fluent also provides the layering remeshing method in dynamic mesh model to govern the mesh reconstruction adjacent to the moving boundaries. The geometry and meshes are created by the grid generation software Gambit 2.2.30, and it should be

noted that the grids at the interface have been refined to precisely predict the free water surface.

The governing equations are solved by using the finite volume method. The second-order upwind discretization is considered for the convection terms. The pressure-velocity coupling is calculated by the NITA (Non-iterative time advancement) - PISO (Pressure implicit with splitting of operators) algorithm compatible with the VOF model, which requires only one global iteration per time step, and reduces solution time significantly.

In Fluent, the symmetry definition is applied for the wave making and absorbing boundaries. The bottom is set as the wall using no-slip conditions. The pressure outlet is considered for the upper boundaries of the computational domain adjacent to the air phase.

2.3 Validation of wave tank

A rectangular wave tank with the flat bottom is set up to validate the capability of the numerical model described in this paper. The tank length is 200 m, and the water depth is 16 m. The maximum displacement of wave maker S_0 is 0.8 m, and the incident wave period T is 3.5 sec. The calculating time step is taken as 0.001 sec.

The numerical results for the time series of wave elevation at the position of x = 30 m and their comparisons with the corresponding analytical solutions are shown in Fig. 2. It can be seen that the numerical results of present model agrees well with the linear solutions after the initial transient effect has diminished.

Figure 3 illustrates the computation for the distribution of wave profile along the tank at t = 23 T. The results obtained by the present method show fairly good agreement with the linear wave solutions. It also can be found that the wave elevations in the numerical prediction are slightly smaller in magnitude than the analytical solutions as the wave propagates in the tank. This difference can be explained by the induced turbulence model in the simulation.

It has been reported that the reflection of the draft of air chamber will create the standing waves with the incident waves. The wave absorbing boundary is replaced by the vertical wall to simulate the standing wave. Figure 4 displays the wave elevation of the point in front of the vertical wall. The period of the standing wave is similar with the incident regular wave. The wave amplitude is about two times higher than that of incident wave, which demonstrates that the current numerical wave tank also can provide the wanted standing waves in front of the vertical wall.

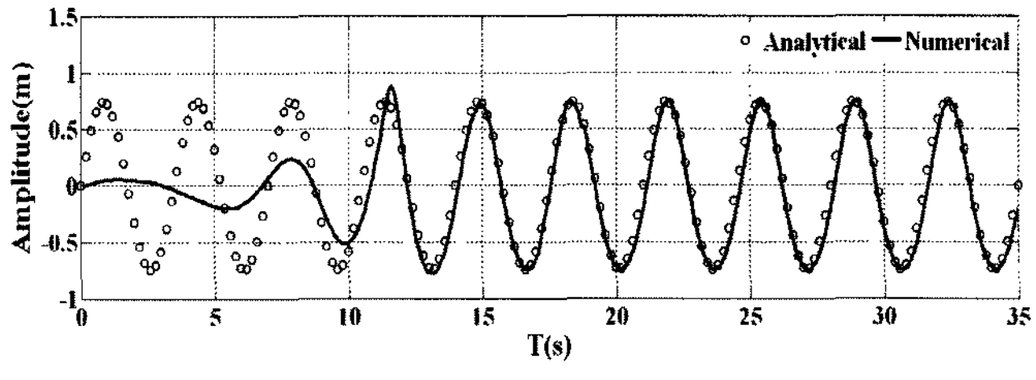

Fig. 2 Time series of wave elevation at the position of x = 30 m

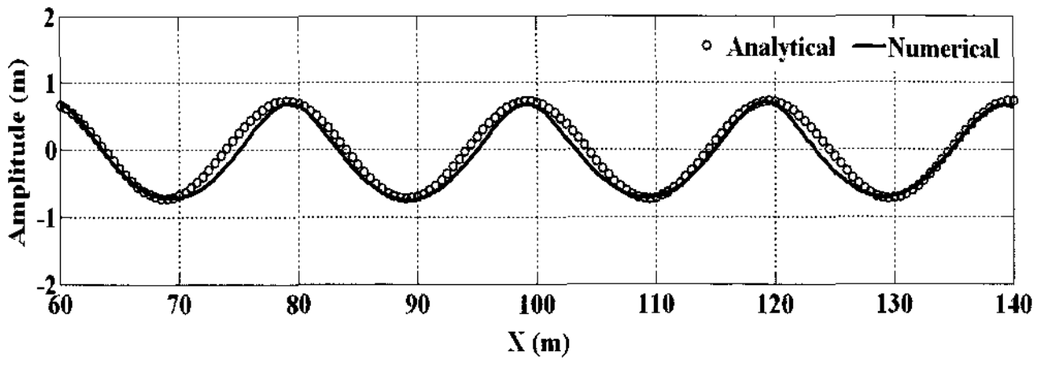

Fig. 3 Comparison of wave profile at t = 23 T

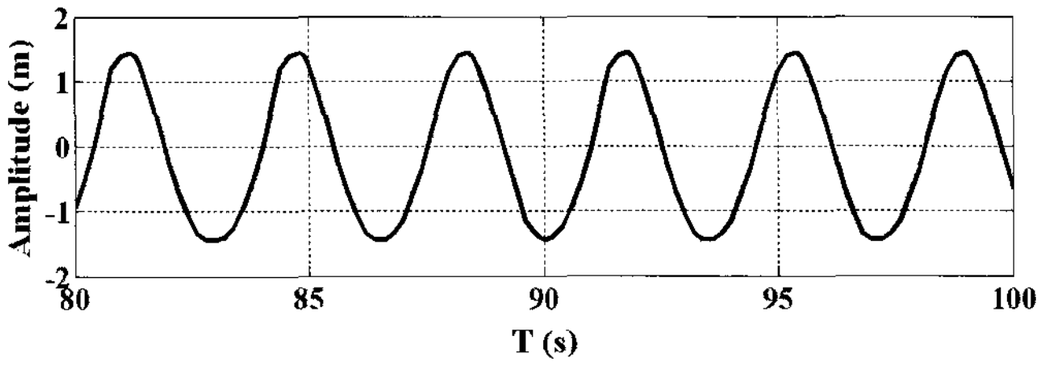

Fig. 4 Distributions of wave profile in one period

All the above numerical results indicate that the 2-D numerical wave tank developed in this paper can generate the desirde propagating regular waves for the engineering applications and investigations of wave field around the air chamber of OWC wave energy converting plants.

3. OWC Chamber

The internal wave field and motion in the OWC air chamber are governed by shape parameters such as the chamber width, thickness of front skirt, size of air duct and the bottom slope. The schematic of fixed OWC air chamber is shown in Fig. 6, where d_s represent the depth of the skirt, l_s the thickness of chamber, l_f the chamber width, l_d the air duct diameter. θ_s denotes the slope angle of bottom, and d_w the mean water depth.

In the present study, the chamber is fixed at an end of the numerical tank and the wave maker system at the other end. The tank length is 320 m while the water depth is set as 16 m. The period of incident linear wave varies from 3.5 sec to 10 sec within the wave amplitude a_0 = 0.5 m. Four cases with various testing conditions summarized in Table. 1 are

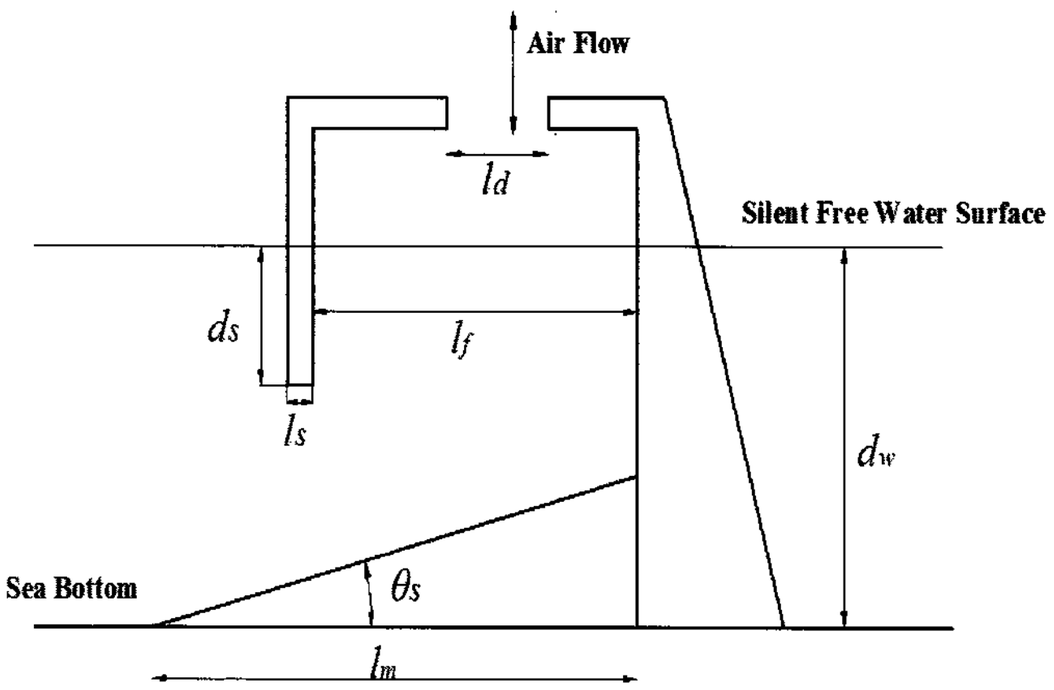

Fig. 5 Schematic of OWC air chamber

Table 1 Testing cases of various shape parameters

Case	l_f(m)	l_s(m)	d_s(m)	l_d(m)	l_m(s)	θ_s(deg.)
01	1.5	1.0	2.5	1.5	23.0	26.0
02	3.0	1.0	2.5	3.0	23.0	26.0
03	1.5	2.0	2.5	1.5	23.0	26.0
04	6.0	1.0	3.5	1.5	23.0	26.0

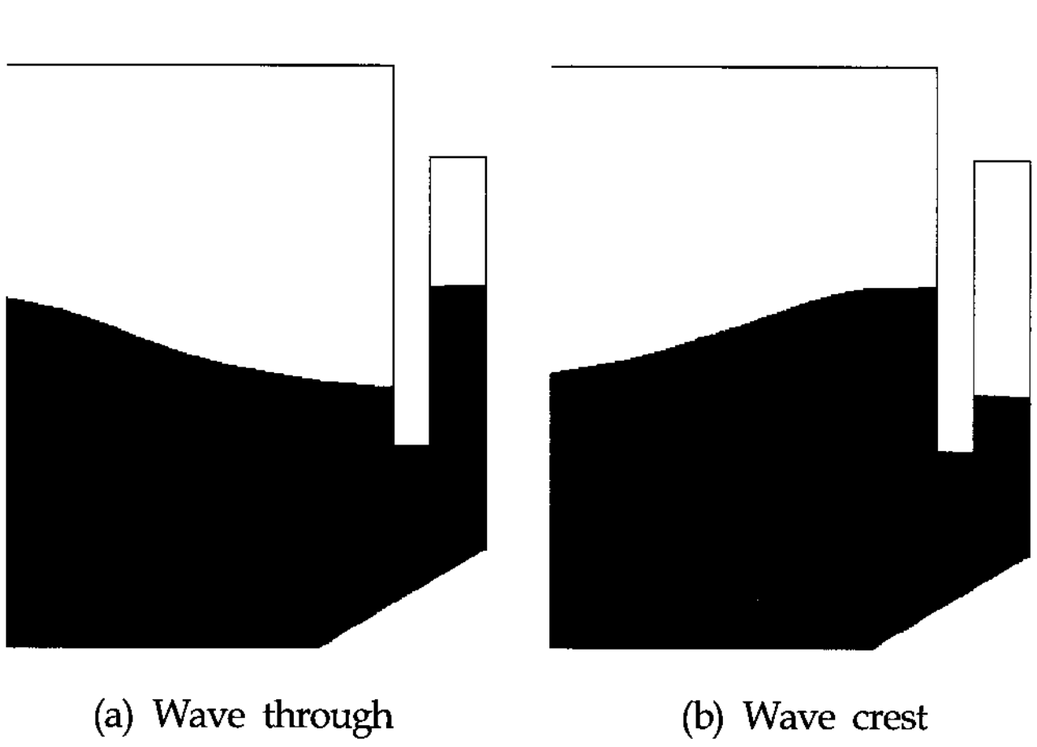

(a) Wave through (b) Wave crest

Fig. 6 Typical wave field distributions in air chamber

studied to compare with the experimental results and demonstrate the effects of the shape parameters. In the first three cases, l_f equals to l_d, which means that the top of chamber is open without any covers.

4. Results and discussion

The typical wave field distributions in the air chamber are calculated. As shown in Fig. 6 (a), the wave trough reaches the chamber, the free surface in the chamber is higher than the water level in front of the skirt, and the water column

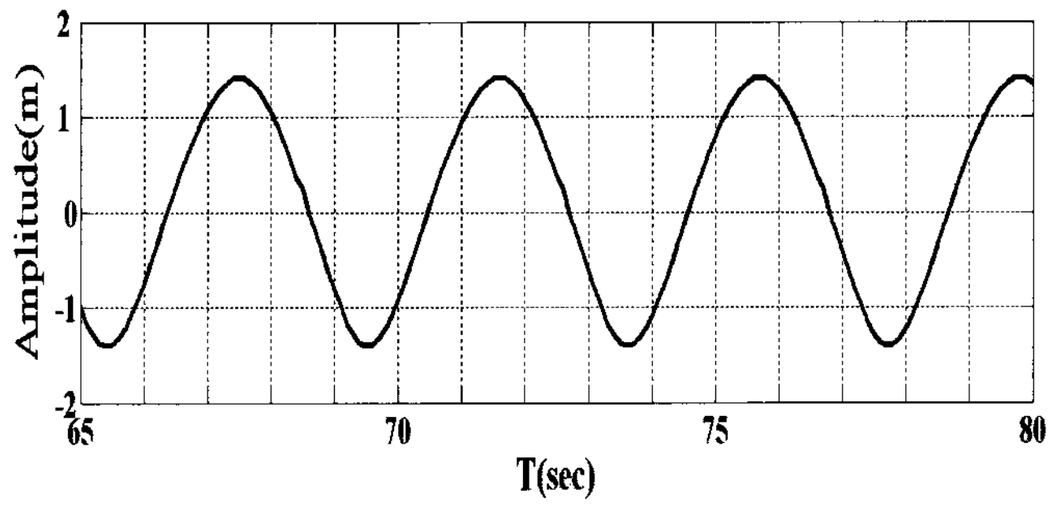

Fig. 7 Water elevation in the air chamber for Case 01, T = 4 s

will fall down. When the wave crest arrives, the water head will raise the water free surface in the chamber seen in Fig. 6 (b). The vertical moving characteristics of the water column shows agreement with that observed in the corresponding experiments.

The water surface elevation in the air chamber of Case 01 for the incident wave period T = 4.0 s is shown in Fig. 7. It can be seen that the oscillating period of water column in the air chamber is about 4.0 sec, which is equal to the incident wave period. Otherwise, the amplitude of water column vertical motion is 2.82 times higher than the incident wave amplitude, which is induced by the resonant effects of air chamber.

The airflow motion and wave energy absorption has relations with the water column oscillation in the chamber. Therefore, it is valuable to investigate the elevating amplitude of water surface to demonstrate the effects of corresponding parameters on the wave power conversion.

The computational dimensionless relative wave amplitude a/a_0 with respect to the incident wave period for Case 01 is given in Fig. 8 (a), where a is the oscillating amplitude of water column in the chamber. The experiment results are also compared in Fig. 8 (a) and agree well with the simulation. It is evident that the relative amplitude varies along the incident wave periods. The peak occurs at around T = 4.5 sec. and the value converges to about 2.1 when the wave period approaches to infinity because of the standing wave formation in front of the chamber skirt.

The numerical results with a larger chamber length in Case 02 are shown in Fig. 8 (b). The tendency of relative amplitude variation is similar with Case 01. The resonant peak value shifts towards the longer period while the magnitude of the amplitude decreases in short period range. The effects of the chamber length are obvious in the water column motion.

The comparison between the simulated prediction and experimental data for a larger skirt thickness in Case 03 are shown in Fig. 8 (c). The numerical resonance peak is a little higher than that of experimental results and shifts to a longer

wave period. The predicted peak value and relative amplitude convergence are a little smaller than those in Case 01, which is similar with the laboratorial results.

The chamber has a cover with the air duct in Case 04. The relative amplitude distribution plotted in Fig. 8 (d) is evidently different from that without the cover. There is no obvious peak

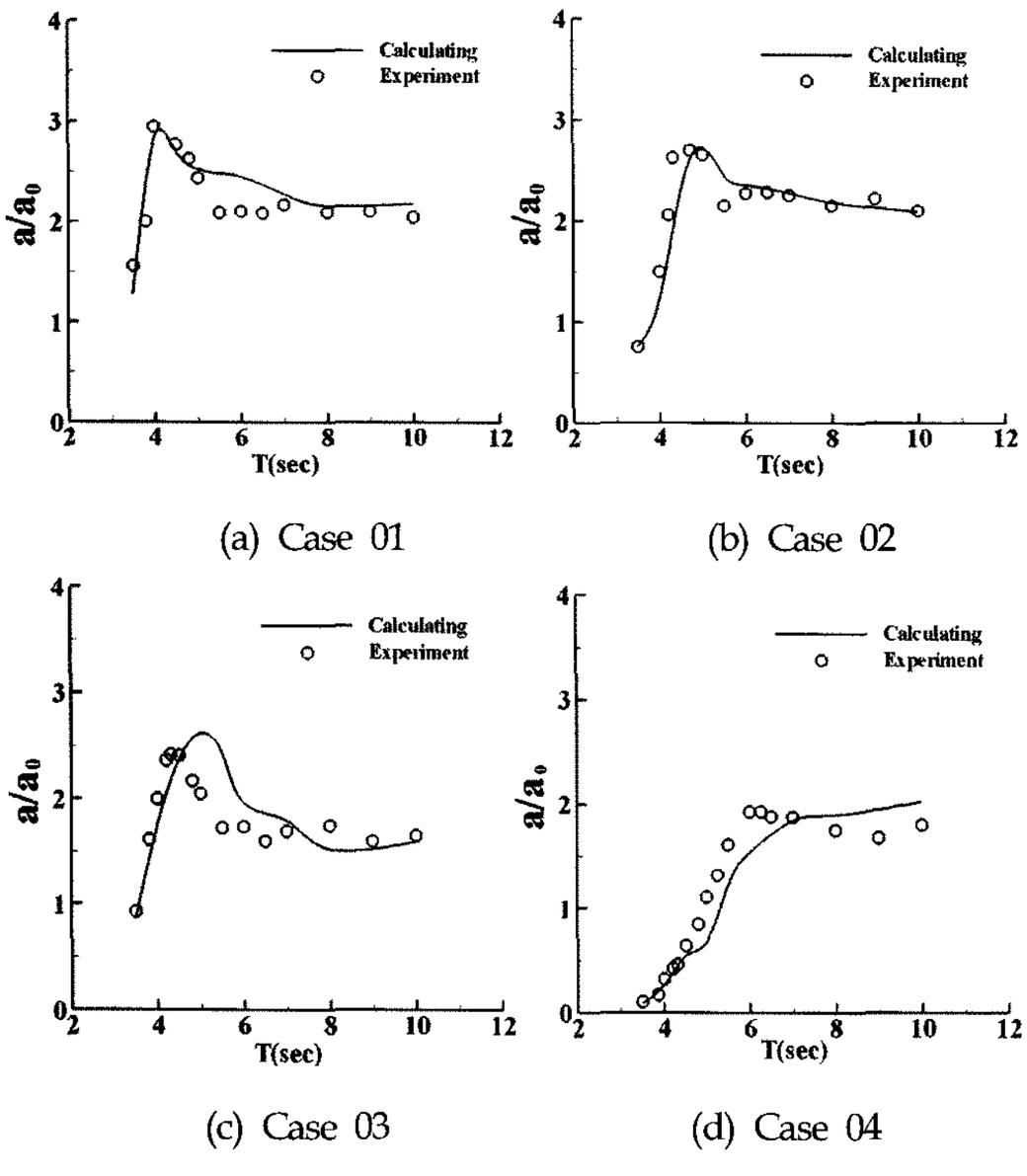

(a) Case 01 (b) Case 02

(c) Case 03 (d) Case 04

Fig. 8 Relative wave amplitude distribution

value along the incident wave periods. It can be found that the computational results are smaller than the measured data before resonant wave period and then slightly higher than the experimental data as the period becomes larger.

In general, all the above numerical predictions show reasonably good agreements with the experimental results and the numerical wave tank can be utilized in the investigation for the wave field in the OWC air chamber. The shape parameters such as the chamber length, front skirt thickness and air duct size have the effects on the oscillating water column motion and wave energy absorption.

5. Conclusions

A 2D numerical wave tank based on the commercial CFD software Fluent 6.2.16 using VOF model has been developed to simulate the wave propagation in this paper. The RANS equations, standard turbulence model and dynamic mesh technology were employed in the present model. The computational regular waves have been validated with the linear solutions.

The relative amplitude distributions of the water column elevation in the chamber with respect to the incident wave period have been calculated and show reasonably good agreements with the experimental results. It can be found that the shape parameters such as the chamber length, front skirt thickness and air duct size all have the effects on the oscillating water column motion and wave energy absorbing capability of the chamber for OWC plants. The results also indicate that the present numerical wave tank can be applied in the corresponding investigation to provide more valuable information of the wave energy conversion.

Acknowledgements

This research was financially supported by Korea Ministry of Maritime Affairs and Fisheries through Korea Ocean Research & Development Institute. The experimental data was also provided by KORDI. All the support is gratefully acknowledged.

References

Evans, D.V. (1982). "Wave-Power Absorption by Systems of Oscillating Surface Pressure Distributions," Journal of Fluid Mechanics, Vol 114, pp 481-499.

Falnes, J. (1980). "Radiation Impedance Matrix and Optimum Power Absorption for Interacting Oscillators in Surface Waves," Applied Ocean Research, Vol 2, pp 45-55.

Hong, D.C., Hong, S.Y. and Hong, S.W. (2004). "Numerical Study on the Reverse Drift Force of Floating BBDB Wave Energy Absorbers," Ocean Engineering, Vol 31, pp 1257-1294.

Hirt C.W., Nichols B.D. (1981). "Volume of Fluid (VOF) Method for the Dynamics of Free Boundaries," Journal of Computational Physics, Vol 39, pp 201-225.

Hong, K.Y., Shin, S.H., Hong, D.C., Choi, H.S. and Hong, S.W. (2007). "Effects of Shape Parameters of OWC Chamber in Wave Energy Absorption," In Proceedings of the Seventeenth International Offshore and Polar Engineering Conference, Lisbon, Portugal, Vol 1, pp 428-433.

Liang, X.G., Sun, P.Y. and You, Y.G. (2003) "Performance Experiment of Shanwei 100kW Wave Power Station's Air-room (in Chinese)," Ocean Engineering, Vol 21, pp 113-116.

Sommerfeld, A. (1949). "Partial Differential Equation in

Physics," Academic Press, New York.

Wang, D.J. (2002). "Analytical and Experimental Investigation on the Hydrodynamic Performance of Onshore Wave-power Devices," Ocean Engineering, Vol 29, pp 871-885.

You, Y. (1993) "Hydrodynamic Analysis on Wave Power Devices in Near-shore Zones," Journal of Hydrodynamics, Ser. B, Vol 5, pp 42-54.

2007년 10월 4일 원고 접수
2008년 1월 21일 최종 수정본 채택